# Selective Microwave Wireless Power Transfer to Sensors Embedded in Concrete at Sub-wavelength Spacing using Electromagnetic Time-reversal Technique

**Baidenger Agyekum Twumasi[1,2], Jia-Lin Li[1], Faith Kwaku Deynu[2], Ebenezer Tawiah Ashong[2], Christian Dzah[2], and Dustin Pomary[2]**

[1]School of Resources and Environment
University of Electronic Science and Technology of China, Chengdu, China
btwumasi@htu.edu.gh, jialinli@uestc.edu.cn

[2]Dept. of Electrical and Electronic Engineering
Ho Technical University, Ho, Ghana
fdeynu@htu.edu.gh, eashong@htu.edu.gh, chdzah@htu.edu.gh, dpomary@htu.edu.gh

***Abstract –*** Wireless power transfer has become a trending research area for remotely transferring power. This paper presents the numerical simulation study of selective wireless power transfer to closely spaced wireless sensors embedded in reinforced concrete. A selective microwave wireless power transfer is achieved at a 10 mm separation between tightly-coupled monopole antennas (wireless sensor antennas). Both tightly-coupled wireless sensors operate at 2.45 GHz, hence beating the diffraction limit at $\lambda/12$ with the incorporation of additional scatterers in the reinforced concrete environment. The main objective is to realize selective wireless power transfer to wireless sensors with sub-wavelength separation (closely spaced) to which one makes the power request. Here, the presence of meta-structures creates some randomness serving as scatterers in the use of the electromagnetic time-reversal technique which enhances the spatial refocusing beyond the diffraction limit. This implies that the focal spot is less than half of the carrier wavelength at the operating frequency. At any time that one of the tightly-coupled sensor antennas sends a power request, power will be transferred to it alone. Cases of dry concrete with and without reinforced bars have been studied with electromagnetic time-reversal techniques for the closely spaced sensors embedded in concrete.

***Index Terms –*** electromagnetic time reversal, sensors, super-resolution, wireless power transfer.

## I. INTRODUCTION

There is increasing demand for wireless devices for various applications such as wireless power transfer [1–4] and electronic toll collection systems [5]. Antennas play crucial roles in wireless power transfer hence the need for an optimum design. In [6], the authors proposed the design of a dipole antenna with matching network using genetic algorithm (GA) optimization. The antenna designed in [6] comprised of a loaded wire dipole and matching network, in which loads and matching network were optimized by the GA in order to enhance the antenna's performance. In [7], an orthogonally integrated hybrid antenna for intelligent transportation systems was proposed. The authors in [1] studied a near field wireless power transfer to sensors embedded in concrete under different scenarios. However, the action distance for this system is not large. Many wireless devices in the era of the internet of things need to be powered and kept on to perform their intended functions. Most of these devices run on batteries which need to be replaced after they run down or get trickle charged in their active service life. In the literature, numerous methods for charging such batteries to enable them to stay in active service over prolonged periods have been proposed.

Wireless power transfer has gained increasing attention in recent years due to the need to continuously power wireless sensors used for various critical monitoring applications. For example, in [3] the authors designed and optimized a robust concrete embedded antenna and minimized the influence of the background material on the energy transfer efficiency to monitor the health of civil structures. In [8], a proof of concept for near field communication for powering sensors in concrete is studied, where the sensors were deeply buried in the concrete. Here, the effect of re-enforcement bars was not considered. Wireless sensors for health monitoring of civil structures can be buried inside the concrete during the construction phase or after the construction to report the health of the civil structure [9]. In [9], power transmission to sensors embedded in reinforced

*Submitted On: June 28, 2023*
*Accepted On: June 21, 2024*



https://doi.org/10.13052/2024.ACES.J.390410

concrete structures is presented. The study considered a single antenna embedded in the concrete structure. Nevertheless, to obtain accurate and timely information on the health of civil structures, multiple sensors will be required.

With the need to monitor civil structures in space constrained environments, embedding closely spaced sensors will be necessary and a super resolution method for transmissions is much desired. This article presents a numerical simulation study which explores the realization of selective wireless power transfer to closely spaced wireless sensors embedded in reinforced concrete for structural health monitoring applications.

## II. ELECTROMAGNETIC TIME-REVERSAL WIRELESS POWER TRANSFER

The electromagnetic time-reversal (EMTR) technique which has been widely applied in acoustic has found wide applications in electromagnetics as well. It has been used in medical imaging, target detection [10], wireless power transfer [11], wireless transmission using pulse shaping [12], power wave forming [13] and telecommunications [14] among others.

The EMTR technique is characterized by spatial and temporal focusing effects. In electromagnetic time reversal, the more complex the medium is with scatterers resulting in reverberation and reflections (multipath), the better the focusing effect. Such complex scattering medium helps to increase the aperture of the antenna time-reversal mirror (TRM). The TRM is enabled to collect the scattered fields, record, flip in time and then transmit back into the same medium from the TRM positioned outside the concrete. The time-reversed waves are found to converge back to the source where the initial transmission originated if the medium is reciprocal [15]. This is even more precise and can be exploited for selective focusing on closely spaced antennas. It is evident that the EMTR technique has been used in various applications in literature but not much research has been done on its application to wireless power transfer to tightly-coupled sensors embedded in concrete with reinforcement bars. In [11], a single-channel TRM is employed as a novel method of wireless power transfer to a moving target in a reverberant medium. EMTR wireless power transfer can surmount the challenges of inductive wireless power transfer such as increasing the action distance and may also reduce the risk of electrocution in its action path since the scattered waveform is not a beam of waves. However, to the best of our knowledge, EMTR wireless power transfer to tightly-coupled monopoles embedded in concrete at separation of 10 mm with reinforcement bars in conjunction with an electromagnetic scatterer plate has not been studied. This article aims to study the selective microwave wireless power transfer to tightly-coupled antennas operating at 2.45 GHz in multiple scattering environments within reinforced concrete structures.

In EMTR wireless power transfer, the receiver transmits a signal to the transmitter, which is then time-reversed and re-transmitted back to the receiver. This process can be described mathematically as:

$$\mathbf{E}_{R(x,y,z,t)} \rightarrow \mathbf{E}_{T(x,y,z,t)} \rightarrow \mathbf{E}_{T(x,y,z,-t)} \rightarrow \mathbf{E}_{R(x,y,z,-t)}, \quad (1)$$

where $\mathrm{E}_{R(x,y,z,t)}$ is the electric field at the receiver at time $t$, $\mathrm{E}_{T(x,y,z,t)}$ is the electric field at the transmitter at time $t$, and $\mathrm{E}_{T(x,y,z,-t)}$ is the time-reversed electric field at the transmitter at time, $-t$.

Using time-reversal symmetry property, we can substitute E(-$t$) for E($t$) in the electromagnetic wave equation to obtain:

$$\nabla^2\mathbf{E} - \mu_0\varepsilon_0\partial^2\mathbf{E}/\partial t^2 = 0, \quad (2)$$

$$\nabla^2\mathbf{E} - \mu_0\varepsilon_0\partial^2\mathbf{E}/\partial(-t)^2 = 0, \quad (3)$$

$$\nabla^2\mathbf{E} + \mu_0\varepsilon_0\partial^2\mathbf{E}/\partial t^2 = 0. \quad (4)$$

These equations describe the behavior of the time-reversed electric field in air medium during EMTR wireless power transfer. However, this equation alone is not sufficient to calculate the exact behavior of the electric field during EMTR wireless power transfer. A more detailed analysis, which considers the specific geometry of the transmitter and receiver, is needed to derive more accurate equations for this process. The electromagnetic wave equation in a concrete environment can be derived by modifying the wave equation in a vacuum to consider the presence of a medium with a non-zero permittivity and permeability. In general, the electromagnetic wave equation in a medium can be written as:

$$\nabla^2\mathbf{E} - \mu\partial^2\mathbf{E}/\partial t^2 - \mu\partial\left(\mu^{-1}\partial\mathbf{E}/\partial t\right)/\partial t = 0, \quad (5)$$

where $\mathbf{E}$ is the electric field, $\mu$ is the permeability of the medium, and $\varepsilon$ is the permittivity of the medium. The second and third terms on the left-hand side of (5) consider the effect of the medium on the propagation of electromagnetic waves.

In a concrete environment, the permeability and permittivity of the medium can be different from those in a vacuum. In general, the permeability of concrete is close to that of free space (i.e., $\mu \approx \mu_0$), while the permittivity can be significantly higher (i.e., $\varepsilon > \varepsilon_0$). Therefore, the electromagnetic wave equation in a concrete environment can be written as:

$$\nabla^2\mathbf{E} - \mu_0\varepsilon\partial^2\mathbf{E}/\partial t^2 - \mu_0\partial\left(\varepsilon_r\varepsilon_0^{-1}\partial\mathbf{E}/\partial t\right)/\partial t = 0, \quad (6)$$

where $\varepsilon_r$ is the relative permittivity (or dielectric constant) of the concrete, which describes how much the permittivity of the concrete differs from that of free space.

## III. DESIGN OF ANTENNA TIME-REVERSAL MIRROR (ATRM)

For structural health monitoring of concrete structures, there will be the need for embedding wireless

sensors near some concrete structures due to space constraints for structural health monitoring and related applications. Due to this, the study of selective focusing of microwave wireless power transfer to embedded tightly-coupled sensors is necessary. Electromagnetic time reversal with spatial focusing properties promises to help realize such selective transfer of power to such tightly-coupled sensors embedded in concrete structures. Therefore, this study focuses on the study of selective wireless power transfer from antennas located outside the concrete structure to tightly-coupled antennas embedded in the concrete structure. The tightly-coupled sensors are denoted by two tightly-coupled monopoles both operating at 2.45 GHz with a separation of 10 mm.

Firstly, two tightly-coupled monopoles are designed to represent the antennas of the wireless sensors embedded in concrete. The two tightly-coupled wire monopole antennas have a separation distance of 10 mm and are positioned on the same ground plane with a radius of 150 mm. Both monopole antennas operate at 2.45 GHz. The optimized height of each monopole is 28 mm. Figure 1 shows the structure of the designed tightly-coupled monopole antennas. The optimum height of these monopole antennas was realized through parameter sweeping study.

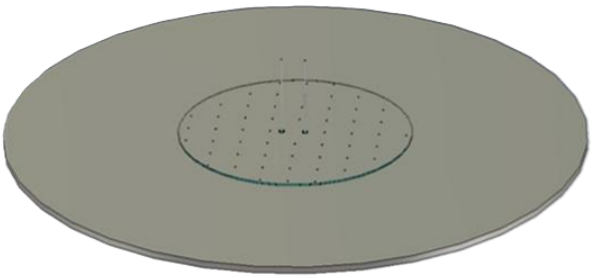

Fig. 1. Tightly-coupled monopole antennas on a large ground plane.

Secondly, we propose the design of a dual-band antenna TRM operating at 2.45 GHz and 5.2 GHz to be used in a wireless power transfer application as TRM to wireless sensors embedded in concrete at 2.45 GHz. It consists of a single-layer substrate ($\varepsilon_r = 2.65$, $\tan\delta = 0.003$) etched with round-end bowtie shaped patch made of copper placed at alternate sides of a 49 mm $\times$ 43 mm substrate having a thickness of 0.8 mm and fed by a coaxial feed line. The bowtie antenna evolved from the conventional microstrip bowtie antenna as discussed in [16]. The initial design of the bowtie antenna was based on the design equation in [16]. After the initial design, the antenna was modified to have a probe feedline. The antenna design was then fine-tuned through numerical simulations. The rounded bowtie antenna is closely related to the conventional one hence the resonance frequency of the patch bowtie antenna for its dominant mode can be derived following the equations in [16] as:

$$f_r = 1.152\frac{c}{L^2\sqrt{\varepsilon_{eff}}}\left(\frac{(W+2\Delta L)+(S+2\Delta L)}{(W+2\Delta L)+(W_c+2\Delta L)}\right), \quad (7)$$

$$\Delta L = \frac{0.412h\left(\varepsilon_{eff}+0.3\right)}{\left(\varepsilon_{eff}-0.258\right)}\left(\frac{\frac{W+W_c}{2h}+0.262}{\frac{W+W}{2h}+0.813}\right), \quad (8)$$

$$e_{eff} = \left(\frac{e_r+1}{2}\right)+\left(\frac{e_r-1}{2}\right)\left(\frac{24h}{W+W_c}+1\right)^{-\frac{1}{2}}. \quad (9)$$

The guided wavelength of the bowtie antenna can be obtained as:

$$\lambda_g = \frac{\lambda_0}{\sqrt{\varepsilon_{eff}}}. \quad (10)$$

The effective side length is expressed as [16]:

$$a_{eff} = a + \frac{h}{\sqrt{e_{eff}}}. \quad (11)$$

The final dimensions of the antenna were optimized using HFSS. The optimum size of the substrate used is 30 mm $\times$ 30 mm and 0.8 mm thickness. The proposed antenna TRM has slots etched on the radiator and metallic scatterers at both sides of the substrate. The other parameters of the proposed antenna TRM are as follows: the flare angle is 130 degrees, the patch on the left-hand side has a radius of 18.768 mm, and the dimensions of the rectangular slot on the left patch is 1.5 mm by 18.678 mm. The patch on the right-side has a radius of 18.760 mm and its rectangular slot has dimensions of 1.5 mm by 19.00 mm. The microstructures (slots) etched on the patch have radii of 0.30 mm and 0.80 mm with a separation of 0.40 mm between them as shown in Fig. 2.

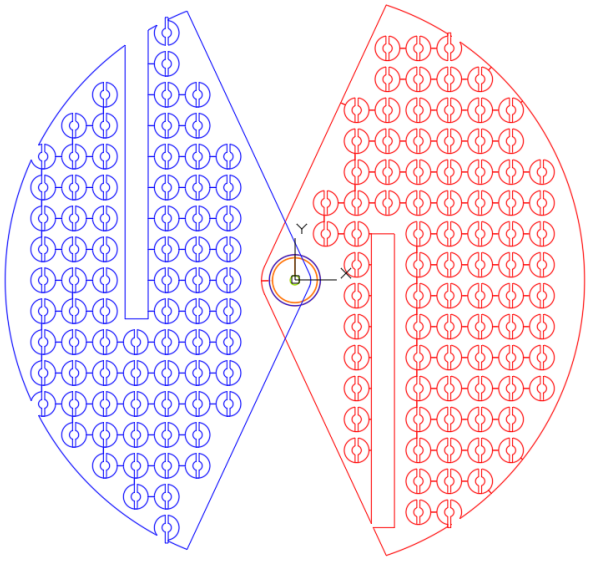


Fig. 2. Layout of the antenna time-reversal mirror.

## IV. DISCUSSIONS OF ANTENNA TRM SIMULATION AND EXPERIMENTAL RESULTS

A prototype of the fabricated bowtie antenna is depicted in Fig. 3. The simulated and measured reflection coefficient of this demonstrator are shown in Fig. 4. The reflection coefficient of the dual-band bowtie antenna with scatterers on both radiators and substrate is below -10 dB from 2.295 GHz to 2.505 GHz resulting in 210 MHz measured bandwidth in the lower operating band (2.45 GHz). For the upper band (5.2 GHz), a measured -10 dB impedance bandwidth of 735 MHz was recorded for frequencies ranging from 4.71 GHz to 5.445 GHz. From Fig. 4, the simulated results for this antenna show that the reflection coefficient is below -10 dB from 2.34 GHz to 2.56 GHz resulting in 240 MHz bandwidth at the lower operating frequency (i.e. 2.45 GHz).

Again, the reflection coefficient is less than -10 dB from 4.75 GHz to 5.54 GHz resulting in 790 MHz bandwidth with the return loss reaching 12.20 dB at 5.2 GHz. We observed that there are some discrepancies between the simulated and measured results. This can be attributed to losses of the coaxial feedline (cable) used for the measurement, the influence of the SMA connector and the unbalanced feed structure of the antenna TRM as well as non-ideal environmental conditions and fabrication uncertainties.

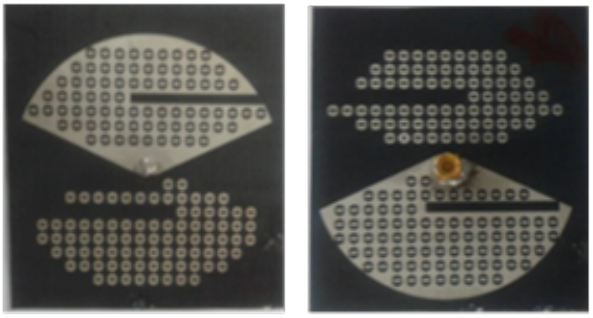

(a) (b)

Fig. 3. Photograph of antenna TRM: (a) front and (b) back.

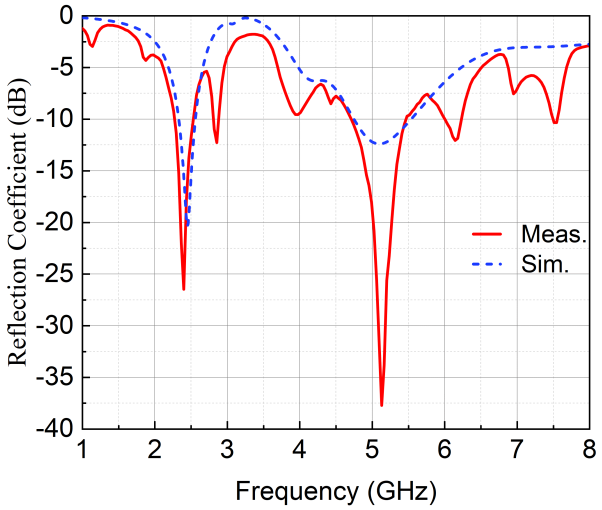


Fig. 4. Simulated and measured $S_{11}$ of the TRM.

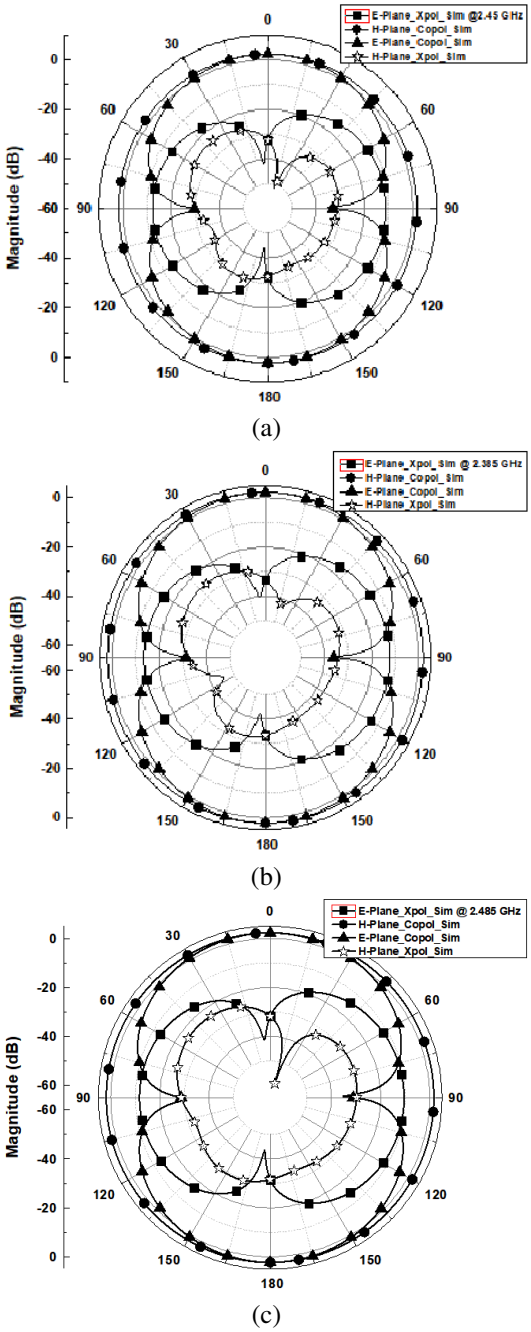


Fig. 5. Simulated radiation patterns of antenna TRM at (a) 2.45 GHz, (b) 2.385 GHz, and (c) 2.485 GHz.

The simulated radiation performance of the proposed antenna at the lower band is shown in Figs. 5 (a-c). It shows simulated radiation performance at 2.385, 2.45 and 2.485 GHz, respectively, all showing typical dipole radiation patterns.

The antenna TRM was also characterized for radiation performance for the upper band resonating at 5.2 GHz and two other frequencies within its operating bandwidth. The radiation patterns are shown in Figs. 6 (a-c) at the frequencies indicated. The measurement setup of the bowtie antenna TRM is shown in Fig. 7.

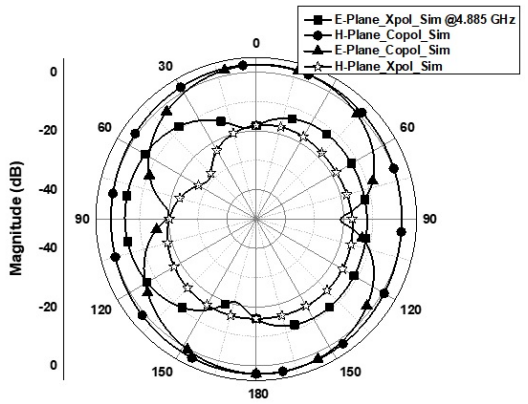


(a)

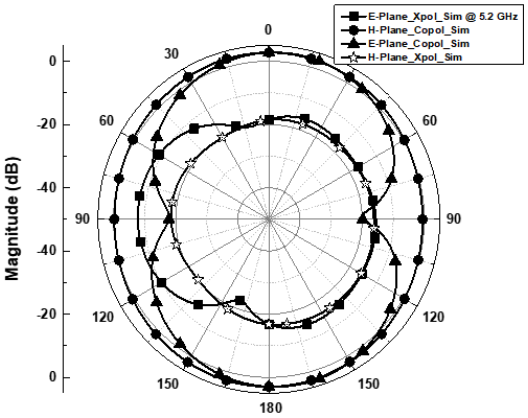


(b)

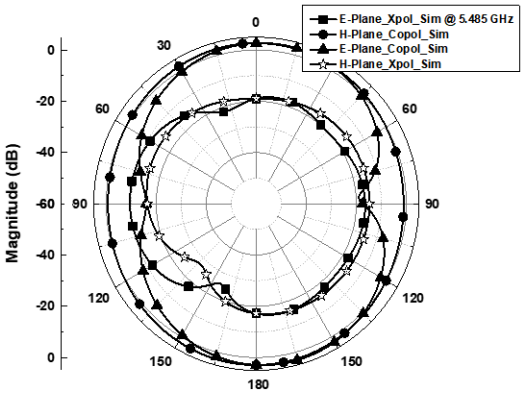


(c)

Fig. 6. Radiation characterization (simulated) of bowtie antenna TRM at (a) 4.885 GHz, (b) 5.2 GHz, and (c) 5.485 GHz.

Fig. 7. Measurement setup of the bowtie antenna TRM.

The scatterers on the bowtie antenna distract the flow of shield current on the radiators serving as perturbation structures on the patch radiators which changes the direction of flow of these currents.

Hence a form of near-field scatterers on the bowtie antennas analogous to the near-field metal wire medium arranged at sub-wavelength scale. The size of these scatterers is much smaller than the size of the antenna radiator implying that these slots will resonate at a far higher frequency. From the observed radiation patterns, it shows that the microstructure scatterers have enhanced the radiation performance of the antenna TRM by decreasing the cross-polarization levels. The resulting high cross polarization discrimination decreases any unwanted field components which is a desired feature of an antenna TRM. This enhances the focusing properties based on the evanescent wave reciprocity principles resulting in super-resolution realizations when used with some wire medium/microstructure array of scatterers in the near field of the transmitting antenna since evanescent waves experience exponential decay. A method of enhancing its propagation to the far field is necessary, hence the techniques adopted.

The simulated reflection coefficient of the tightly-coupled monopole antenna is shown in Fig. 8. Opti-

mum performance is realized when the length of the monopole antenna is 28 mm. The two tightly-coupled wire monopole antennas have separation of 10 mm with a ground plane of 150 mm in radius and both operate at 2.45 GHz. The optimized height of each monopole is 28 mm.

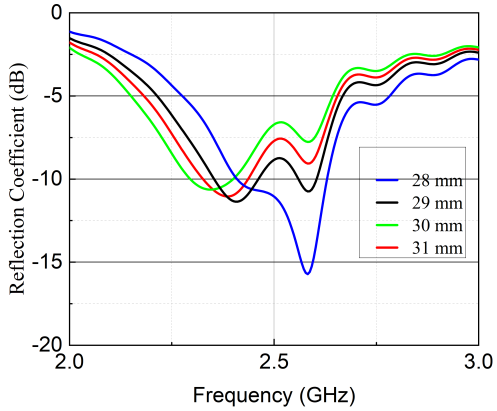


Fig. 8. Simulated reflection coefficient ($S_{11}$) of the tightly-coupled monopole antennas.

## V. NUMERICAL SIMULATION OF SELECTIVE WIRELESS POWER TRANSFER TO SENSORS EMBEDDED IN CONCRETE

Figure 9 shows the setup of the tightly-coupled antennas embedded in concrete without re-enforcement bars. In this setup, the antenna TRMs with slots are positioned outside the concrete structure and the tightly-coupled monopole antennas/sensors requesting power are embedded in the concrete structure. The antenna TRM has a face-to-face separation distance of 300 mm.

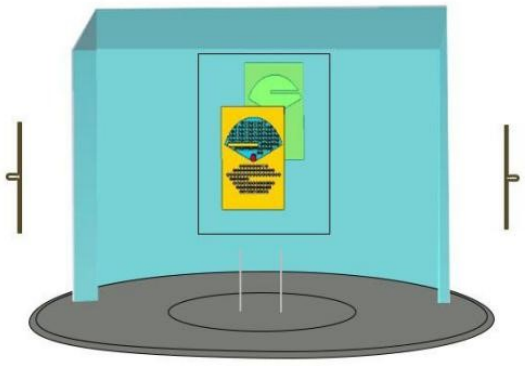

Fig. 9. Setup for concrete without re-enforcement bars with embedded tightly-coupled monopoles.

Four TRMs were used to provide power transfer to the embedded tightly-coupled antennas. Table 1 shows performance comparison between the proposed antenna and other studies. The proposed antenna compares favorably with other works. The concrete material has a dielectric constant of 4.5 with a loss tangent of 0.011. A block of concrete was modelled with dimensions of 200 mm by 200 mm and a height of 150 mm.

For this study, three setups have been considered and numerically studied. In Fig. 9, there are no re-enforcement bars and scatterers. In Fig. 10, re-enforcement bars (rebars) are embedded in the concrete. The re-enforcement bars are made of iron rods with the properties of a lossy metal. The iron rods' diameter is 16

Table 1: Performance comparison of the proposed antenna and other works

| Ref | Dimension (mm) | Bandwidth (GHz) | Frequency (GHz) | Gain (dBi) |
|---|---|---|---|---|
| [17] | 50×50 (etched on both copper layers) | NA | 2.4, 3.5, 5.3 | 1.8, 1.5, 4.5 |
| [16] | 110×50 (etched on single copper layer) | NA | 0.9 / 1.8 1.25, 2.1 | 3.5/ 4.4 3.9, 5.1 |
| [18] | 45 × 65 (edged on both copper layers) | 4.0-6.8 | 4.2, 5.5, 6.6 | 11.08 at 5.5 GHz |
| **This work** | **49 × 43** | **2.295-2.505, 4.71-5.445** | **2.45, 5.2** | **3.7, 3.0** |

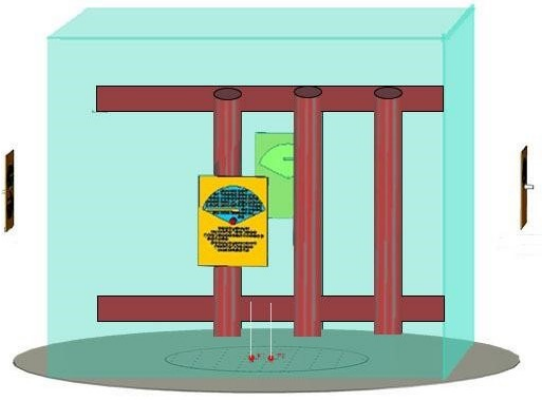

Fig. 10. Re-enforced concrete structure with embedded monopole antennas and rebars and surrounding TRMs.

mm with a length of 200 mm and arranged as shown in Fig. 10.

Further, the concrete is embedded with rebars and additional two plates of electromagnetic scatterers close to the iron rods.

The electromagnetic scatterer plate is designed with a microwave substrate with copper strips of the length of a wavelength at the operating frequency and sub-wavelength separation arranged on one side of the microwave substrate. The dielectric constant of the microwave substrate used is 2.65.

Figure 11 shows the unit cell of the proposed scatterer embedded in the concrete structure. The corresponding dimensions are listed in Table 2. The complete 15×15 scatterer plate is shown in Fig. 12.

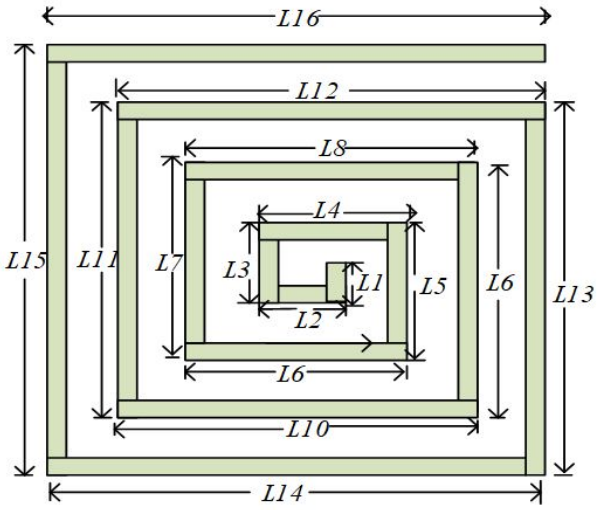


Fig. 11. Unit cell of the scatterer showing its respective dimensions.

Table 2: Dimensions of the scatterer

| Parameter | Value (mm) | Parameter | Value (mm) |
|---|---|---|---|
| *L1* | 3.00 | *L10* | 8.625 |
| *L2* | 3.625 | *L11* | 9.25 |
| *L3* | 4.25 | *L12* | 9.875 |
| *L4* | 4.875 | *L13* | 10.50 |
| *L5* | 5.5 | *L14* | 11.125 |
| *L6* | 6.125 | *L15* | 11.75 |
| *L7* | 6.75 | *L16* | 12.375 |
| *L8* | 7.375 | *Width of strip* | 1.00 |
| *L9* | 8.00 | | |

All numerical simulations were carried out using Computer Simulation Technology (CST). MATLAB was used to reverse the signals for the time-reversal signal re-transmission. An initial channel-sounding pulse was

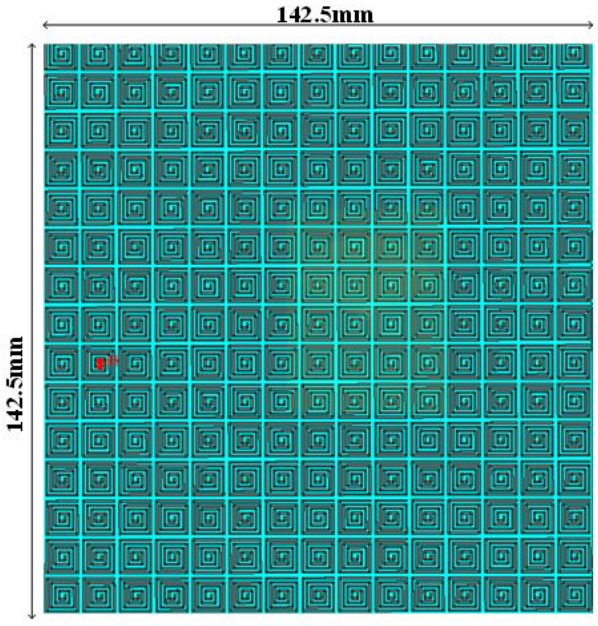


Fig. 12. The 15 × 15 array scatterer plate.

transmitted from the antenna/sensor making the power request. This signal (total field) is then received by four antennas (ATRM), flipped in time using the MATLAB program and then re-transmitted from the TRM into the concrete structure using CST. The complete setup including the additional electromagnetic scatterers in the form of a scatterer plate is shown in Fig. 13.

The objective is to improve the scattering of the electromagnetic waves to realize super-resolution wireless power transfer. This structure consists of an array of coiled copper strips with their unit cell as depicted in Fig. 11 and the scatterer plate as shown in Fig. 12. The

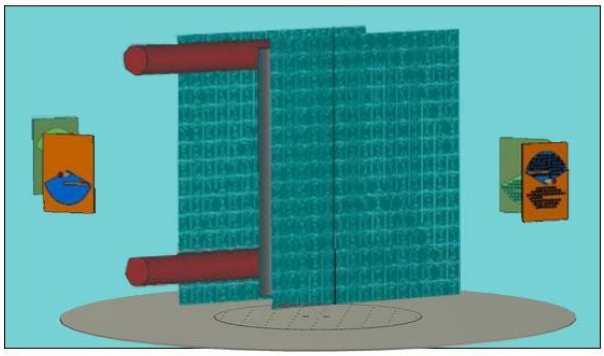

Fig. 13. Setup of re-enforced concrete with additional scatterers embedded in concrete.

scatterers and the rebars embedded in the concrete have helped to enhance the effective aperture of the embedded monopole antennas hence yielding super-resolution performance using the time-reversal technique.

## VI. NUMERICAL SIMULATION RESULTS AND DISCUSSIONS OF SUPER-RESOLUTION WIRELESS POWER TRANSFER IN CONCRETE

The numerical simulation results of the three cases studied are presented in this section. Figure 14 (a) shows the time signals plot of the setup of wireless power transfer into the concrete without rebars and the scatterer plates. The results in Fig. 14 (a) show that this setup failed to realize super-resolution wireless power transfer for the tightly-coupled monopoles as the magnitude of the voltage signal received by the two monopoles is nearly the same in magnitude. There is no clear distinction showing the attainment of at least a 50% difference in the magnitude of the amplitude of the time signals received by the two tightly-coupled antennas [19]. Figure 14 (b) shows the electric field distribution for this case.

It can be observed from Fig. 14 (b) that the two monopole antennas have almost the same level of electric field distribution around them and no distinction as to which monopole transmitted the channel-sounding pulse. The two monopole antennas have been denoted on the time signal plots as Port 1 and Port 2, respectively, denoting monopole antenna 1 and monopole antenna 2. It can be observed from Fig. 15 (a) that the magnitude of the time signals between antenna 1 (Port 1) and antenna 2 (Port 2) shows at least a 50% difference in magnitude of the time signals between the time 2-4 ns, where the time from 0-2 ns can be regarded as

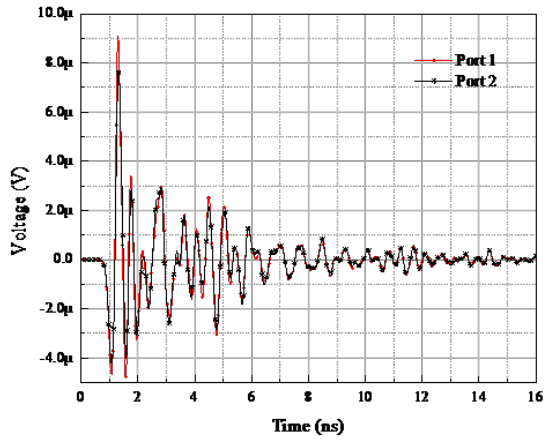


(a)

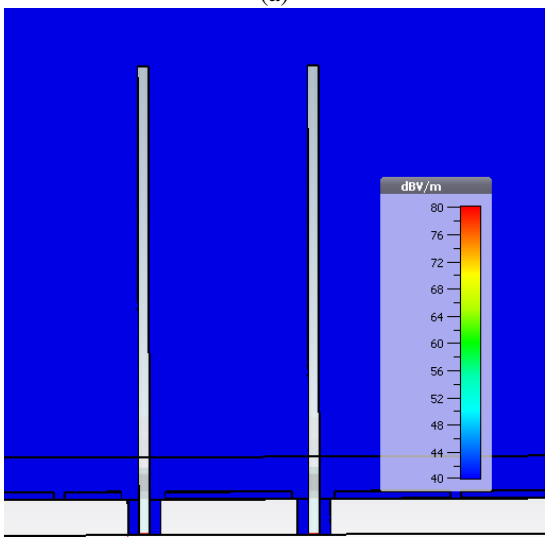


(b)

Fig. 14. Results for concrete without re-enforcement and additional scatterers: (a) time signal plot and (b) electric field distribution on the tightly-coupled antennas.

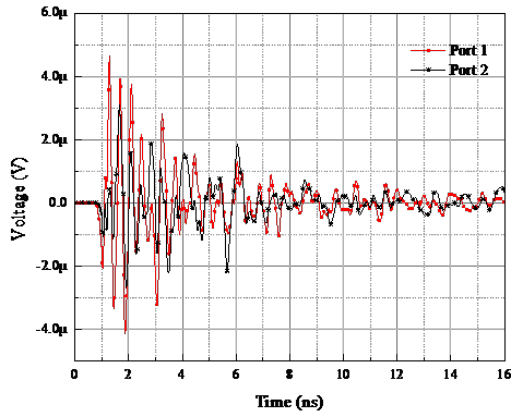


(a)

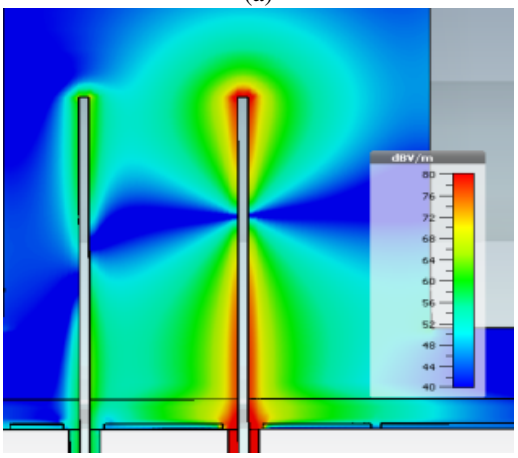


(b)

Fig. 15. Results for the two tightly-coupled monopoles embedded in concrete with enforcement bars: (a) time signal diagram of the two monopoles and (b) electric field distribution.

the early time response and also after 4-16 ns, regarded as the late time response hence not considered in the analysis. From the time signals plots and the electric field distribution shown in Fig. 15 (b), it is observed that this scenario has realized super-resolution wireless power transfer to the tightly-coupled monopole antennas. The monopole antenna that initially transmitted making the power request has a stronger electric field distribution on it as compared to the other that did not transmit. Figure 15 shows the time signals plot and the electric field distribution, where additional electromagnetic scatterers have been embedded close to the rebars. It can be seen from Fig. 15 that between 2 and 4 ns, this study has realized super-resolution wireless power transfer between the tightly-coupled monopoles with a separation distance of 10 mm. The electric field distribution shown in Fig. 15 (b) demonstrates a clear distinction between the tightly-coupled antennas with the receiving antenna (Port 1) showing a stronger field distribution than Port 2.

For the first time, to the best of our knowledge, we propose a figure of merit (FoM) for evaluating microwave wireless power transfer into concrete structures using the EMTR technique for tightly-coupled monopoles. This can be derived based on the efficiency of power transfer and the robustness of the technique to variations in the properties of the concrete medium.

The power transfer efficiency ($\eta$) is a key metric for evaluating the performance of wireless power transfer systems. It is defined as the ratio of the power received by the receiver ($P_R$) to the power transmitted by the transmitter ($P_T$), or $\eta = P_R/P_T$. In the context of microwave wireless power transfer into concrete structures using the EMTR technique, $\eta$ can be calculated based on the power received by the receiver during the time-reversal process and the power transmitted by the receiver during the forward transmission. The properties of concrete, such as its relative permittivity ($\varepsilon_r$) and loss tangent ($\tan\delta$), can vary significantly depending on factors such as moisture content, temperature and the presence of reinforcing materials (rebars). To ensure reliable wireless power transfer using the EMTR technique, the system must be robust to such variations in concrete properties. One way to evaluate the robustness of the technique is to calculate the sensitivity of the power transfer efficiency to changes in the concrete properties. This can be expressed as a relative change in efficiency ($\eta$) per unit change in $\varepsilon_r$ or $\tan\delta$.

Based on these considerations, a possible FoM for evaluating microwave wireless power transfer into concrete structures using the time-reversal technique can be defined as:

$$\mathrm{FoM} = \eta / \left(\mathrm{s}^2_{\varepsilon_\mathrm{r}} + \mathrm{s}^2_{\tan\delta}\right), \tag{12}$$

where $\mathrm{s}_{\varepsilon_\mathrm{r}}$ and $\mathrm{s}_{\tan\delta}$ are the sensitivities of the power transfer efficiency to changes in $\varepsilon_\mathrm{r}$ and $\tan\delta$, respectively. This FoM considers both the power transfer efficiency and the robustness of the system to variations in concrete properties.

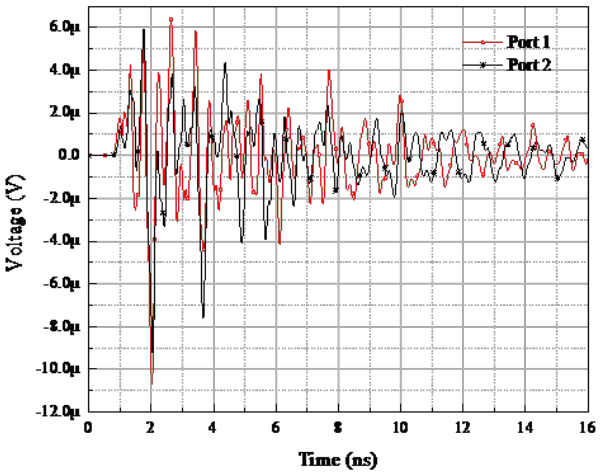


(a)

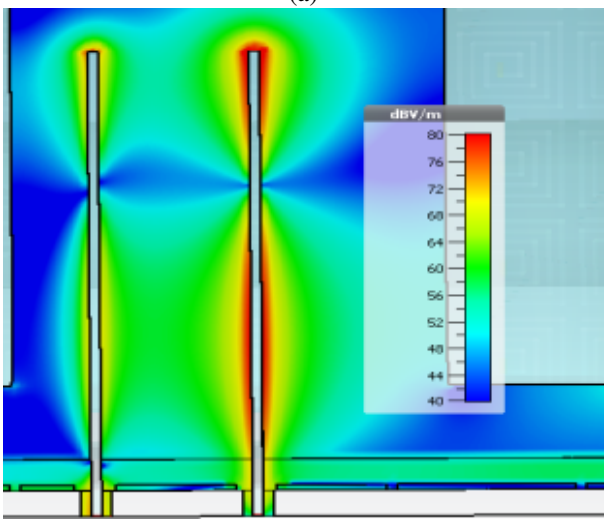


(b)

Fig. 16. Results for the two tightly-coupled monopoles embedded in concrete with enforcement bars and additional scatterers: (a) time signals plot and (b) electric field distribution of the tightly-coupled antennas embedded in the concrete.

A higher FoM indicates a more efficient and robust wireless power transfer system. For wireless power transfer of closely spaced monopole antennas, the following leads to the derivation of a FoM for the system.

The spacing between the closely spaced monopole antennas embedded into concrete can have a significant impact on the efficiency of wireless power transfer. In general, the spacing should be as small as possible to

maximize the coupling between the monopole antennas, while avoiding interference between them.

Based on these considerations, a possible FoM for evaluating microwave wireless power transfer into concrete structures using the electromagnetic time reversal technique for closely spaced monopoles embedded into concrete can be defined as:

$$FoM = \frac{\eta}{s_{\varepsilon_r}^2 + s_{tan\delta}^2 + \frac{\lambda}{\delta}}, \tag{13}$$

where $\lambda$ is the wavelength of the transmitted signal and $\delta$ is the spacing between the monopole antennas. The last term in the equation considers the practical constraint on the spacing between the monopole antennas. A higher FoM indicates a more efficient and robust wireless power transfer system for a given spacing between the monopole antennas. Note that the specific values of the sensitivities and the practical constraint term may vary depending on the specific application and the design of the wireless power transfer system.

In many applications, it is desirable to limit the extent of power transfer to a localized region of the concrete structure. The degree of localization of power transfer can be evaluated using metrics such as the spatial distribution of the power density, or the ratio of the power density in the target region to the total power density received by the receiver.

Based on these considerations, a possible FoM for evaluating microwave wireless power transfer into concrete structures using the electromagnetic time reversal technique for closely spaced monopole antennas embedded into concrete can be defined as:

$$FoM = \frac{\eta}{s_{\varepsilon r}^2 + s_{tan\delta}^2} \times \frac{(P_T, P_R)_{target}}{(P_T, P_R)_{total}}, \tag{14}$$

where $s_{\varepsilon r}$ and $s_{\tan\delta}$ are the sensitivities of the power transfer efficiency to changes in $\varepsilon_r$ and $\tan\delta$, respectively, and $(P_T, P_R)_{\text{target}}$ and $(P_T, P_R)_{\text{total}}$ is the total transmitted and received power in the target region and the total transmitted and received power, respectively. This FoM considers the power transfer efficiency, robustness of the technique and degree of localization of power transfer. A higher FoM indicates a more efficient, robust and localized wireless power transfer system.

## VII. CONCLUSION

In this paper, a super-resolution microwave wireless power transfer to antennas embedded in concrete has been studied. Furthermore, the operating environment of the tightly-coupled monopole antennas has been studied with its effect on the selective wireless power transfer realization. The case of receiving power by one tightly-coupled monopole antenna using electromagnetic time reversal coupled with scatterers has shown that the antennas' environment can affect it constructively or destructively depending on the technique used. With the EMTR technique, the scatterers have constructively aided the realization of selective wireless power transfer of $1/12\lambda$ of the operating frequency at 2.45 GHz within the industrial, scientific and medical (ISM) band. This study has shown some promising potential in selective wireless power transfer with the electromagnetic time reversal, which will help transfer power to tightly-coupled antennas in space-constrained applications for wireless trickle charging of wireless sensors for civil health structural monitoring. In addition, a figure of merit (FoM) has been defined for the first time to characterize wireless power transfer into concrete structures using the electromagnetic time-reversal technique for tightly-coupled monopoles (sensors).

## ACKNOWLEDGMENT

This work was supported in part by the National Science Foundation of China (NSFC) under grant No. 62271105 and in part by Ho Technical University Research Fund (HTURF).

## REFERENCES

[1] R. H. Bhuiyan, M. R. Islam, J. M. Caicedo, and M. Ali, "A study of 13.5-MHz coupled-loop wireless power transfer under concrete and near metal," *IEEE Sens. J.*, vol. 18, no. 23, pp. 9848-9856, 2018.

[2] Y. Peng, W. Qi, Y. Chen, R. Mai, and U. K. Madawala, "Wireless sensor power supply based on eddy currents for structural health monitoring," *IEEE Trans. Ind. Electron.*, vol. 71, no. 7, pp. 1-10, 2023.

[3] T. Bigler, G. Kovács, A. Treytl, and R. Windl, "NFC for powering sensors in concrete," in *IEEE Symposium on Emerging Technologies and Factory Automation, ETFA*, pp. 1355-1358, 2020.

[4] S. H. Lee, M. Y. Kim, B. S. Lee, and J. Lee, "Impact of rebar and concrete on power dissipation of wireless power transfer systems," *IEEE Trans. Ind. Electron.*, vol. 67, no. 1, pp. 276-287, 2020.

[5] L. T. Tran, C. D. Khuat, and L. V. Phi, "A wideband, high gain and low sidelobe array antenna for modern ETC systems," *Applied Computational Electromagnetics (ACES) Journal*, vol. 38, no. 5, pp. 333-342, 2023.

[6] K. Kayalvizhi and S. Ramesh, "Design and analysis of reactive load dipole antenna using genetic algorithm optimization," *Applied Computational Electromagnetics (ACES) Journal*, vol. 35, no. 3, pp. 279-287, 2020.

[7] S. Syedyusuff, R. Subramaniam, and R. Vijay, "Orthogonally integrated hybrid antenna for intelligent transportation systems," *Applied Computational Electromagnetics (ACES) Journal*, vol. 36, no. 5, pp. 519-525, 2021.

[8] G. Castorina, L. Di Donato, A. F. Morabito, T. Isernia, and G. Sorbello, "Analysis and design of a concrete embedded antenna for wireless monitoring applications [antenna applications corner]," *IEEE Antennas Propag. Mag.*, vol. 58, no. 6, pp. 76-93, 2016.

[9] J. R. Tenório Filho, J. Goethals, R. Aminzadeh, Y. Abbas, D. E. V. Madrid, V. Cnudde, G. Vermeeren, D. Plets, and S. Matthys, "An automated wireless system for monitoring concrete structures based on embedded electrical resistivity sensors: Data transmission and effects on concrete properties," *Sensors*, vol. 23, no. 21, p. 8775, 2023.

[10] B. A. Twumasi and J. L. Li, "Numerical simulation study on bowtie antenna-based time reversal mirror for super-resolution target detection," *J. Electr. Eng.*, vol. 70, no. 3, pp. 236-243, 2019.

[11] F. Cangialosi, T. Grover, P. Healey, T. Furman, A. Simon, and S. M. Anlage, "Time reversed electromagnetic wave propagation as a novel method of wireless power transfer," in *2016 IEEE Wireless Power Transfer Conference, WPTC 2016*, 2016.

[12] S. Ding, S. Gupta, R. Zang, L. Zou, B. Z. Wang, and C. Caloz, "Enhancement of time-reversal subwavelength wireless transmission using pulse shaping," *IEEE Trans. Antennas Propag.*, vol. 63, no. 9, pp. 4169-4174, 2015.

[13] M. Ku, Y. Han, H. Lai, Y. Chen, S. Member, and K. J. R. Liu, "Power waveforming: Wireless power transfer beyond time reversal," *IEEE Trans. Signal Processing*, vol. 64, no. 22, pp. 5819-5834.

[14] A. E. Fouda, F. L. Teixeira, and M. E. Yavuz, "Time-reversal techniques for MISO and MIMO wireless communication systems," *Radio Sci.*, vol. 47, no. 5, 2012.

[15] G. Lerosey, J. De Rosny, A. Tourin, A. Derode, G. Montaldo, and M. Fink, "Time reversal of electromagnetic waves," *Physical Review Letters*, vol. 92, no. 19, p. 193904.

[16] O. W. Ata and M. I. Jawadeh, "Design of a novel split-bowtie slotted multi-resonant antenna," *International Journal of Electrical and Electronic Engineering & Telecommunications*, pp. 1-8, 2022.

[17] Y. Tawk, K. Y. Kabalan, A. El-Hajj, C. G. Christodoulou, and J. Costantine, "A simple multiband printed bowtie antenna," *IEEE Antennas Wirel. Propag. Lett.*, vol. 7, pp. 557-560, 2008.

[18] P. Dhanaraj and S. Uma Maheswari, "Performance analysis of electrically coupled SRR bowtie antenna for wireless broadband communications," *Wireless Networks*, vol. 26, no. 7, pp. 5271-5283, 2020.

[19] H. Tu, S. Xiao, D. Lesselier, and M. Serhir, "Super-resolution characteristics based on time-reversed single-frequency electromagnetic wave," *J. Electromagn. Waves Appl.*, vol. 30, no. 13, pp. 1670-1680, 2016.

**Baidenger Agyekum Twumasi** was born in Nsawam, E/R-Ghana in 1981. He received an H.N.D. in Electrical/Electronic Engineering from Ho Technical University (Ho Polytechnic), Ghana, in 2004, the Master of Engineering degree (MEng.) in Telecommunication Management from the HAN University of Applied Sciences, Arnhem, the Netherlands in 2011, and the Ph.D. degree in Electronic Science and Technology from the University of Electronic Science and Technology of China, Chengdu, China in 2020. He is with the University of Electronic Science and Technology of China (UESTC), China, as a post-doctoral researcher. He has been with the Electrical & Electronic Engineering Department of Ho Technical University (HTU), Ho, in Ghana since February 2008 where he is currently a Senior Lecturer. His current research interests include antennas and propagation, electromagnetic time-reversal applications, wireless power transfer, flexible (wearable) electronics, circuits and systems.

**Jia-Lin Li** was born in October 1972 in Sichuan, China. He received the M.S. degree from the University of Electronic Science and Technology of China (UESTC), Chengdu, China, in 2004, and the Ph.D. degree from the City University of Hong Kong, Hong Kong, in 2009, both in electronic engineering. From September 2005 to August 2006, he was a Research Associate with the Wireless Communication Research Center, City University of Hong Kong, Hong Kong. From September 2009 to April 2021, he was with the School of Physical Electronics, UESTC and initially served as a Lecturer and then a professor. Since May 2021, he has been with the School of Resources and Environment, UESTC. His research interests include microwave/millimeter-wave antennas and arrays, circuits and systems, electromagnetic-wave detection, and imaging.

**Faith Kwaku Deynu** received his MSc. degree in Telecommunication Engineering at HAN University of Applied Sciences, Netherlands in 2011 and his Ph.D. degree in Information and Communication Engineering at University of Electronic Science and Technology of China (UESTC), Chengdu, China. He is currently a Senior Lecturer at Electrical/Electronic Engineering Department of Ho Technical University, Ho, Ghana. His research interests include internet protocol (IP) multimedia subsystems, optical fiber, and power line communication systems.

**Ebenezer Tawiah Ashong** received a B.Sc. degree in Telecommunication Engineering from Kwame Nkrumah University of Science and Technology, Kumasi, Ghana in 2015 and an MEng degree in Electronic Engineering from Hanbat National University, Daejeon, Korea, in 2019. He is currently pursuing a PhD in Electrical and Information Engineering at Seoul National University of Science and Technology, Seoul, Korea. He is currently a Lecturer in the Department of Electrical & Electronic Engineering at Ho Technical University, Ho. His current research interests include antennas and arrays, wireless power transfer, electromagnetic compatibility, measurement and instrumentation, and telecom policy and regulation.

**Christian Dzah** was born in Ho, Volta Region of Ghana in 1977. He obtained his Higher National Diploma (HND) Certificate in Electrical/Electronic Engineering from Ho Polytechnic, Ghana in 2009. He obtained his Bachelor of Science Degree in Electrical/Electronic Engineering from Regional Maritime University, Accra-Ghana, in 2015. In 2019, he obtained his Master of Philosophy Degree in Electrical and Electronic Engineering from the University of Mines and Technology, Tarkwa, Ghana. Currently, he is an Assistant Lecturer in the Department of Electrical/Electronic Engineering, at Ho Technical University, Ghana.

**Dustin Pomary** received his Bachelor of Engineering in Biomedical Engineering from All Nations University, Koforidua, Ghana, in 2017 and his MPhil in Biomedical Engineering at the University of Ghana, Legon, in 2021. His thematic area of study is implants sciences and regenerative engineering. He is currently an Assistant Lecturer in the Department of Electrical & Electronic Engineering at Ho Technical University, Ho, Ghana. His current research interests include implant sciences, regenerative engineering, drug delivery, computational simulation, and biomaterials.